Electronic and atomic structures of a 3×3 surface formed by a binary Sn/Ag overlayer on the Ge(111)c(2×8) surface: ARPES, LEED, and STM studies

Hafiz M. Sohail,* J. R. Osiecki, and R. I. G. Uhrberg
Department of Physics, Chemistry and Biology, Linköping University, S-581 83 Linköping, Sweden
(Received 21 December 2011; revised manuscript received 19 April 2012; published 7 May 2012)

The electronic and atomic structures of a well-ordered 3×3 periodicity of a binary Sn/Ag overlayer on Ge(111) have been studied. The ordered binary overlayer was formed by depositing 0.75 monolayer of Sn on an Ag/Ge(111) $\sqrt{3}\times\sqrt{3}$ surface. Annealing at 330 °C resulted in a low-energy electron diffraction pattern that exhibited sharp spots. A detailed electronic structure investigation was performed by angle-resolved photoelectron spectroscopy. The Sn/Ag/Ge(111) 3×3 surface shows a rich band structure. There are seven bands which are positively identified as 3×3 surface bands, all within 1.5 eV below the Fermi level (E_F). The upper two bands disperse across E_F exhibiting steep almost linear dispersions down to a minimum energy of ≈0.40 eV below E_F at the $\bar{\Gamma}$ point (≈0.30 eV at the $\bar{K}$ point). Constant energy contours have been mapped in the 3×3 surface Brillouin zone (SBZ) in order to study an intriguing split observed in the band structure related to the two upper bands. It turned out that the two upper bands are degenerate along the $\bar{\Gamma}-\bar{K}$ and $\bar{M}-\bar{K}$ symmetry lines of the 3×3 SBZ but separated along $\bar{\Gamma}-\bar{M}$. Scanning tunneling microscopy images obtained at ≈40 K show essentially a hexagonal structure except for a honeycomb structure in a limited bias range imaging empty states. Core-level spectroscopy shows a narrow Sn 4*d* spectrum consistent with the high degree of structural order.

DOI: 10.1103/PhysRevB.85.205409 PACS number(s): 68.47.Fg, 73.20.−r, 68.37.Ef, 79.60.−i

I. INTRODUCTION

Metal overlayers on semiconductor surfaces are important systems that have been extensively studied for several decades. The research effort is, to a large extent, motivated by the formation of well-ordered, self-assembled, one- and two-dimensional structures that are of both fundamental and technological interest. A few examples are Ag, Au, Sn, In, and Pb on Si or Ge surfaces, which all exhibit well-ordered structures.[1–8] Most of the studies have been devoted to deposition of a single metal, while binary combinations of metals have been given very little attention so far. Studies of binary overlayers have mostly involved the addition of small amounts of a second metal onto a well-ordered periodic substrate formed after deposition of the initial metal on an Si or Ge surface.[9–19] One example of a binary system is the combination of 0.3 monolayer (ML) of Pb and 0.6 ML of Sn on Si(111) which shows a $\sqrt{7}\times\sqrt{3}$ superstructure.[14] Another example is a small amount of Au (0.19 ML) or Cs on Ag/Si(111) $\sqrt{3}\times\sqrt{3}$ which results in a $\sqrt{21}\times\sqrt{21}$ periodicity.[15,16] Further examples are small amounts of noble metals (Ag, Au) or alkali metals (K, Cs) on the Ag/Ge(111) $\sqrt{3}\times\sqrt{3}$ or Ag/Si(111) $\sqrt{3}\times\sqrt{3}$ surfaces, respectively, which result in various well-ordered reconstructions.[17,18] In a recent publication, adsorption of In on the Au/Si(111) $\sqrt{3}\times\sqrt{3}$ surface was reported to result in a sharpening of the $\sqrt{3}\times\sqrt{3}$ low-energy electron diffraction (LEED) pattern, and significant changes of the electronic structure in terms of shifts to higher binding energies were observed.[19] These examples indicate that there are most likely several interesting new surface structures to be explored for various binary overlayers on the surfaces of the elemental semiconductors. However, the increased complexity of a binary system is quite demanding when it comes to analysis of experimental results and to investigations of the systems by theoretical methods. In this paper, we have chosen Ag and Sn as the two metallic elements. One monolayer of Ag on the clean Ge(111)c(2×8) surface results in a well-ordered Ag/Ge(111) $\sqrt{3}\times\sqrt{3}$ surface after annealing. This surface was used as a substrate for deposition of Sn as the second metal. The choice of Sn was, to some extent, triggered by the large number of studies of the Sn/Ge(111) $\sqrt{3}\times\sqrt{3}$ and Sn/Ge(111) 3×3 surfaces that have appeared in the literature. Both the Ge(111)/Ag and Ge(111)/Sn systems are well studied,[17,20–22] which provides a solid base of knowledge for the analysis of binary Sn/Ag overlayers.

In this paper, we present results for an Sn/Ag binary system obtained by depositing 0.75 ML of Sn on an Ag/Ge(111) $\sqrt{3}\times\sqrt{3}$ surface. By annealing the surface, the periodicity transformed from the initial $\sqrt{3}\times\sqrt{3}$ to a 3×3 ordering as verified by LEED. The electronic structure of the surface was studied using angle-resolved photoelectron spectroscopy (ARPES), resulting in the identification of seven surface bands following the new 3×3 periodicity. These bands have been mapped along the high-symmetry directions $\bar{\Gamma}-\bar{M}-\bar{\Gamma}$ and $\bar{\Gamma}-\bar{K}-\bar{M}$ of the 3×3 surface Brillouin zone (SBZ). The 3×3 periodicity has been verified over an exceptionally large $k_{\parallel}$ range for some bands, covering up to seven 3×3 SBZs. The upper surface bands cross the Fermi level, and the 3×3 surface is thus metallic. In order to investigate the atomic structure of the surface, a detailed bias-dependent STM study was performed at low temperature. At most biases, the images show features in a hexagonal arrangement, while a honeycomb structure appears clearly in the empty-state images at some biases. Most of the features in the STM images are quite extended and are therefore associated with a rather large number of atoms. In our study, we found that the proper Sn coverage necessary to produce a 3×3 surface was in the range 0.6–0.8 ML. Sn depositions well below or above this range result in ordered surface reconstructions other than 3×3, depending on the precise amount of Sn and annealing conditions.

II. EXPERIMENTAL DETAILS

Angle-resolved photoelectron spectroscopy measurements were performed at the MAX-lab synchrotron radiation facility in Lund, Sweden, while STM studies were done at Linköping University, Sweden. The experimental station at beamline I4, located at the MAX-III storage ring, was used for the photoemission study. This beamline provides linearly polarized light in the energy range of 14 to 160 eV. All sample preparations and measurements were conducted in the UHV system (base pressure $<1.5\times10^{-10}$ Torr) consisting of an analysis chamber and a preparation chamber. The preparation chamber was equipped with a sputter gun, Ag and Sn evaporators, a residual gas analyzer (RGA), and a quartz crystal thickness monitor. During the deposition of Ag and Sn, the pressure was $<4\times10^{-10}$ Torr. The analysis chamber was equipped with a Specs Phoibos 100 analyzer with a 2D detector, i.e., the raw data consist of maps of the intensity of emitted electrons as function of both energy (y axis) and emission angle (x axis).

Ge(111) samples were cut from an n-type single-crystal wafer (Sb doped, 7–10 Ω cm). The samples were degreased *ex situ* and cleaned *in situ* by repeated Ar^+-ion (1 keV) sputtering and annealing (730 °C) cycles. These cycles were repeated until a well-ordered Ge(111)c(2×8) surface could be verified by LEED. In order to prepare the Ag/Ge(111) $\sqrt{3}\times\sqrt{3}$ surface, 1.1 ML of Ag was evaporated at room temperature onto clean Ge(111)c(2×8). Annealing at 330 °C for 2 min resulted in a well-ordered $\sqrt{3}\times\sqrt{3}$ periodicity. The Ag/Ge(111) $\sqrt{3}\times\sqrt{3}$ surface was used as substrate for the deposition of Sn. In this study, 0.75 ML of Sn was deposited at room temperature. Subsequent annealing at 330 °C for 2 min resulted in a well-defined 3×3 periodicity as confirmed by LEED. The 3×3 surface appeared at 280 °C and remained up to 350 °C. The LEED optics of the analysis chamber was used to orient the sample azimuthally in order to probe the high-symmetry directions in the ARPES study. In this paper, we present ARPES data from the Sn/Ag/Ge(111) 3×3 surface, resulting in a mapping of the surface bands along the $\bar{\Gamma}-\bar{M}-\bar{\Gamma}$ and $\bar{\Gamma}-\bar{K}-\bar{M}$ directions of the 3×3 SBZ as well as constant energy contour maps. The band mapping was done at a photon energy of 30 eV, at an energy resolution of ≈20 meV, and an angular resolution of 0.3°. A Ta foil in electrical contact with the sample was used to obtain an energy reference for the Fermi level (E_F) for the ARPES data.

The STM study was performed in a UHV system consisting of an analysis chamber and a preparation chamber. The main components of the preparation chamber were similar to those of the system used for the ARPES study, while the analysis chamber was equipped with a LEED optics and a variable-temperature STM from Omicron. The STM was fitted with a tungsten tip, produced by electrochemical etching, and cleaned *in situ* by e^--beam heating. Low-energy electron diffraction and STM were used to verify the sample quality after the preparation of each surface, i.e., after the preparation of the Ge(111)c(2×8), the Ag/Ge(111) $\sqrt{3}\times\sqrt{3}$, and the final Sn/Ag/Ge(111) 3×3 surface. The STM experiments were run in constant current mode (200 pA). Empty- and filled-state images of the 3×3 surface were recorded at room temperature and at a temperature of ≈40 K. Even though LEED showed well-defined spots from the Sn/Ag/Ge(111) 3×3 surface, it was quite difficult to obtain high-quality STM images. The surface structure was, to a large extent, obscured by streaks due to species moving on the surface or being dragged along by the tip. In order to avoid this situation, a slightly smaller amount of Ag (≈0.8 ML) was deposited onto the Ge surface because of the well-known diffusion of extra Ag atoms on other surfaces, such as Ag/Si(111) $\sqrt{3}\times\sqrt{3}$.[23] The smaller amount of Ag resulted in $\sqrt{3}\times\sqrt{3}+4\times4$ spots in the LEED patterns after annealing, where the appearance of 4×4 spots was taken as experimental evidence that the amount of Ag was actually less than 1 ML.[24] Scanning the Sn/Ag/Ge(111) 3×3 areas formed on this kind of sample resulted in images with fewer streaks.

III. RESULTS AND DISCUSSION

Figures 1(a) and 1(b) show LEED patterns of the Ag/Ge(111) $\sqrt{3}\times\sqrt{3}$ and Sn/Ag/Ge(111) 3×3 surfaces, respectively. It is evident from the sharp spots that the $\sqrt{3}\times\sqrt{3}$ and 3×3 surfaces both exhibit well-ordered periodicities (some spots are labeled in the figures for guidance). There are no other kinds of diffraction spots in either of the two patterns, which indicates that each surface corresponds to a single reconstruction phase. Beside LEED patterns, STM images of the corresponding surfaces are also presented, see Figs. 1(c) and 1(d). They are empty-state, large-scale images (155×155 nm^2) obtained at bias voltages of 2.0 and 1.5 V, respectively. The images in Figs. 1(c) and 1(d) show large terraces on both surfaces. Some smaller islands are present on Sn/Ag/Ge(111) 3×3, see Fig. 1(d). In the case of the $\sqrt{3}\times\sqrt{3}$ surface, the step edges are quite sharp, while in the case of the 3×3 surface, they look a bit rough.

Figure 2 shows the experimental band structure of the Sn/Ag/Ge(111) 3×3 surface along the $\bar{\Gamma}-\bar{K}-\bar{M}$ [Fig. 2(b)] and $\bar{\Gamma}-\bar{M}-\bar{\Gamma}$ [Fig. 2(c)] directions of the 3×3 SBZ. The

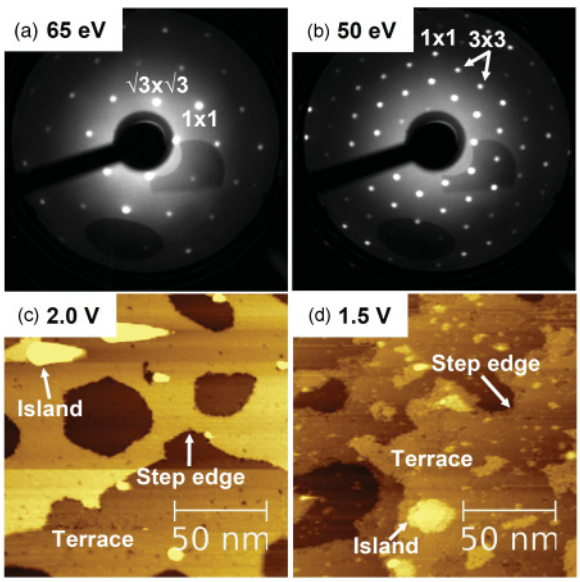

FIG. 1. (Color online) (a) and (b) LEED patterns and (c) and (d) empty-state STM images of the Ag/Ge(111) $\sqrt{3}\times\sqrt{3}$ (at 2.0 V) and Sn/Ag/Ge(111) 3×3 (at 1.5 V) surfaces, respectively. Both LEED and STM data were obtained at room temperature.

1×1 and 3×3 SBZs are shown in Fig. 2(a). The data, on which Figs. 2(b) and 2(c) are based, were obtained at a sample temperature of ≈80 K using a photon energy of 30 eV. Photoemission data obtained at 17, 21.2, and 40 eV resulted in band structures consistent with that derived from the 30 eV data. Figures 2(b) and 2(c) show the second derivative, along the energy axis, of the photoemission intensity on the two-dimensional, energy vs angle, detector of the electron analyzer. A larger magnitude of the second derivative corresponds to a darker color in Fig. 2. We have chosen to show the second derivative of the photoemission intensity to make also weak, but well-defined structures visible. The obvious advantage of using the second derivative is that all bands can be visualized in the same figure, something that is hard to achieve in a grayscale representation of photoemission data with many bands of varying intensity. Several 20°-wide frames have been stitched to cover an extended angle range (−20 to 50°), that has been converted to a $k_{\parallel}$ range of −1.3 to 2.2 Å^{-1}. There are several bands that show a periodicity consistent with the 3×3 reconstruction of the surface. In Fig. 2(b), there are six bands (S_1–S_6), indicated by arrows, that show a periodicity consistent with the $\bar{\Gamma}-\bar{K}-\bar{M}$ direction of the 3×3 SBZ. Along $\bar{\Gamma}-\bar{M}-\bar{\Gamma}$, one can also identify six bands following the 3×3 periodicity, see Fig. 2(c). The experimental band structure is fairly complicated, and it is somewhat difficult to get a clear picture of the various bands. However, by having a closer look, the following bands can be traced across several neighboring 3×3 SBZs. The S_1 band shows steep, almost linear dispersions around the $\bar{\Gamma}$ and the $\bar{K}$ points of the 3×3 SBZ. The energy is ≈−0.40 eV at $\bar{\Gamma}$ and ≈−0.30 eV at $\bar{K}$. From these minima, the S_1 band disperses steeply across the Fermi level. The dispersion of the S_1 band repeats itself across six neighboring SBZs along $\bar{\Gamma}-\bar{M}-\bar{\Gamma}$, as can be seen from Fig. 2(c). A peculiar split of S_1 into two bands can be observed near the Fermi level at various parts along the $k_{\parallel}$ axis in both Figs. 2(b) and 2(c). We return to a discussion of this split at the end of the presentation of the photoemission data.

A second band S_2 in the energy range from −0.3 to ≈−0.6 eV, can also be followed over a large $k_{\parallel}$ range. The magnitude of the second derivative varies across the $k_{\parallel}$ range, which results in a variation of the visibility of the S_2 band in Figs. 2(b) and 2(c). The difficulty to follow the band dispersions across the full $k_{\parallel}$ range, covered by the experimental data, increases for the deeper bands. A third band S_3 exists in the energy range from ≈−0.5 to ≈−0.6 eV, with an upward dispersion from $\bar{\Gamma}$ toward $\bar{M}$ and $\bar{K}$ points. In the right part of Fig. 2(c), a fourth band S_4 is clearly observed in the range from ≈−0.55 to ≈−0.7 eV with dispersion maxima at both $\bar{\Gamma}$ and $\bar{M}$ points. Weak features of a fifth band S_5 can be seen in a narrow energy range around −0.9 eV near the $\bar{\Gamma}$ points of the 3×3 SBZs. Note that the S_5 band shows up clearly at the $\bar{\Gamma}_1$ points along $\bar{\Gamma}-\bar{K}-\bar{M}$. At $\bar{\Gamma}_1$ points, the S_5 band is located within the gap of the projected bulk bands, which makes the band more prominent. Finally, a sixth band S_6 following the 3×3 periodicity can be identified in Fig. 2(c). The S_6 band has minima at the $\bar{\Gamma}$ points of the 3×3 SBZs at an energy of ≈−1.1 eV. From this energy, it disperses steeply upward toward $\bar{M}$, see Fig. 2(c). The S_6 band shows a steep upward dispersion also toward $\bar{K}$, as can be seen in the rightmost part of Fig. 2(b). Bands (S_1–S_6) all show a

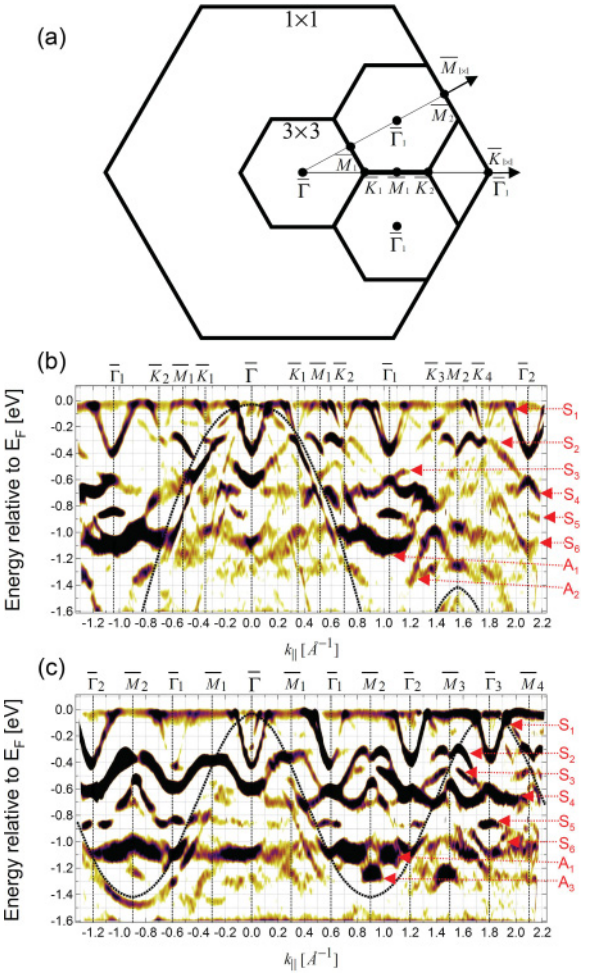

FIG. 2. (Color online) (a) 1×1 and 3×3 SBZs with high-symmetry directions indicated. (b) and (c) Band structure of the Sn/Ag/Ge(111) 3×3 surface obtained by ARPES in the $\bar{\Gamma}-\bar{K}-\bar{M}$ and $\bar{\Gamma}-\bar{M}-\bar{\Gamma}$ directions, respectively, of the 3×3 SBZ using a photon energy of 30 eV while keeping the sample at a temperature of ≈80 K. The figures show the magnitude of the second derivative, obtained along the energy axis, of the photoemission intensity. A darker color corresponds to a larger value. The dashed curves in (b) and (c) show the upper edge of the projected bulk bands.

periodicity consistent with the 3×3 SBZ, the bands exist in the projected bulk band gap, and they show a consistent dispersion for different photon energies (17, 21.2, 30, and 40 eV were used in this study). Based on this, we can conclude that the Sn/Ag/Ge(111) 3×3 surface exhibits at least six characteristic surface state bands.

In the projected bulk band gap near the $\bar{K}$ and $\bar{M}$ points of the 1×1 SBZ, there are additional surface bands. In the deep gap near $\bar{K}_{1\times1}$ (1.045 Å^{-1}), there are two bands labeled A_1 and A_2, see Fig. 2(b). These bands are also present near $\bar{K}_{1\times1}$ on the opposite side of $\bar{\Gamma}$. Near the $\bar{M}_{1\times1}$ points (0.905 Å^{-1}), there are also two bands, see Fig. 2(c). The upper one, A_1 is located in the energy range −1.0 to −1.2 eV. The appearance of this band in the 1×1 projected band gap resembles that of the back-bond state on the clean Ge(111)c(2×8) surface.[25] Finally, there is an indication of a third band A_3 at −1.25 eV at the $\bar{M}_{1\times1}$ point on the positive side of $\bar{\Gamma}$. The dispersions

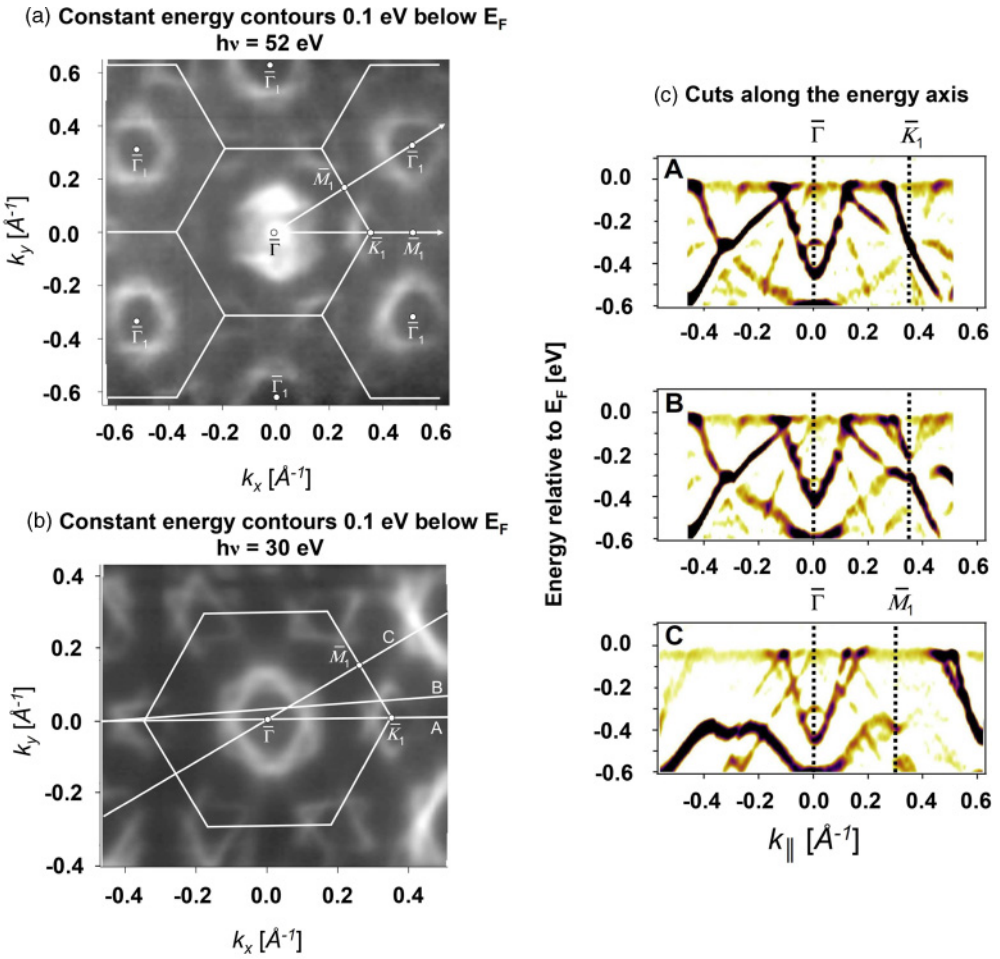

FIG. 3. (Color online) (a) and (b) Constant energy contours at 0.1 eV below E_F obtained from the Sn/Ag/Ge(111) 3×3 surface using a photon energy of 52 and 30 eV, respectively. (c) Band structure along the A, B, and C azimuthal directions defined in (b).

of the bands (A_1–A_3) do not follow the 3×3 periodicity. The origin of these three bands will not be further discussed in this paper.

Figures 3(a) and 3(b) show constant energy contours in the (k_x,k_y) plane at an energy of 0.1 eV below E_F. The contours are shown for two photon energies, 52 eV in Fig. 3(a) and 30 eV in Fig. 3(b). In Fig. 3(a), there are six $\bar{\Gamma}$ points around the central one, as indicated by the superimposed 3×3 SBZs. The contours around each of the six outer $\bar{\Gamma}$ points are a bit diffuse, but a close look reveals that they consist of two reversed triangles, one with a corner pointing in the positive k_y direction and a second triangle with a corner pointing in the opposite direction. A quite different appearance of the constant energy contours is observed near the central $\bar{\Gamma}$ point. The surface band contours are here obscured by strong emission due to a direct bulk transition that occurs close to E_F at 52 eV.[26] The contours obtained around the $\bar{K}$ points at 52 eV are quite weak, but they are clearly revealed using 30 eV, see Fig. 3(b). In similarity with the contours around the $\bar{\Gamma}$ points in Fig. 3(a), the contours around the $\bar{K}$ points in Fig. 3(b) consist of reversed triangles that combine into a starlike shape. The contours at E_F (not shown here) are similar to the ones in Figs. 3(a) and 3(b), but the finer details are less clear.

The observation of two triangular contours implies that there are two surface bands near E_F instead of just one S_1 band. The apparent split of the upper band mentioned earlier, see Figs. 2(b) and 2(c), is a consequence of the existence of two bands. In order to understand more about the observed splitting, three cuts along the energy axis of the three dimensional (E,k_x,k_y) dataset are shown in Fig. 3(c). Panels A, B, and C of Fig. 3(c) correspond to three different azimuthal orientations, as indicated by the lines in Fig. 3(b). Line A is perfectly aligned with the $\bar{\Gamma}-\bar{K}-\bar{M}$ direction. This line crosses the two triangular contours at a (k_x,k_y) point that is equivalent for the two surface bands. As a consequence, there is no split observed near E_F, see panel A of Fig. 3(c). Panel B shows the effect of a slight misalignment, here exemplified by a combination of a small tilt angle and a small azimuthal error, see line B in Fig. 3(b). The band structure along line B shows a clear split near E_F, as is evident in the right part of panel B. However, even in the case of a perfect alignment, the split might be present. This is the situation along the $\bar{\Gamma}-\bar{M}-\bar{\Gamma}$ high-symmetry direction, line C in Fig. 3(b), where the two triangular contours are intersected at different (k_x,k_y) points. A clear split is thus present in the experimental band structure shown in panel C of Fig. 3(c). Based on the cuts through the three dimensional (E,k_x,k_y) dataset, we conclude that the

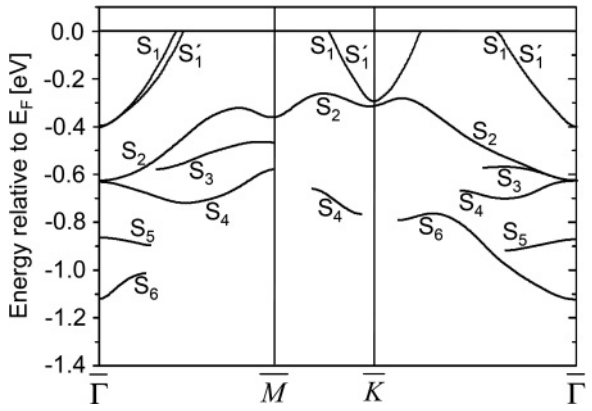

FIG. 4. Schematic band structure of the seven surface states (S'_1, S_1–S_6) identified on Sn/Ag/Ge(111) 3×3.

surface band structure of Sn/Ag/Ge(111) 3×3 consists of two bands near E_F.

The varying visibility of the surface bands across the $k_\parallel$ range makes it difficult to get a clear picture of the dispersions of all the bands in the 3×3 SBZ. We have therefore traced the clearest parts of the experimental 3×3 bands in Fig. 2 and reproduced them in Fig. 4. The resulting plot is a schematic representation of the surface band dispersions along the high-symmetry lines $\bar{\Gamma}-\bar{M}$, $\bar{\Gamma}-\bar{K}$, and $\bar{M}-\bar{K}$ of the 3×3 SBZ. The split of S_1 into two bands is indicated by S'_1. Note that S'_1 only appears between $\bar{\Gamma}$ and $\bar{M}$ since the two bands are degenerate along $\bar{\Gamma}-\bar{K}$ and $\bar{M}-\bar{K}$. With the S'_1 band, there is a total of seven bands (S'_1, S_1–S_6) that follow the 3×3 periodicity.

Figure 5 shows Sn 4*d* and Ge 3*d* core-level spectra obtained from the Sn/Ag/Ge(111) 3×3 surface. The Sn 4*d* core-level spectrum shows essentially a well-resolved spin-orbit doublet with no obvious shifted components. There is an asymmetric tail that can be fitted with a small asymmetry of the Doniach–Šunjić line shape ($\alpha = 0.02$). The asymmetry is consistent with the metallic character of the surface. To obtain a high-quality fit, it is necessary to add a second component at a slightly higher binding energy. The integrated intensity of this component is about 16% of the total Sn 4*d* intensity. It is, however, not really possible to determine the origin of this component. From the wide Gaussian width (0.5 eV) compared to the narrow main component (0.27 eV), one can suspect that the second component is due to Sn atoms at various disordered sites on the surface, not related to the 3×3 structure. Although the percentage varies with the exact fitting parameters used, it gives an idea of the number of Sn atoms contributing to the broad component. The sharpness of the main component indicates that most Sn atoms are located in a well-defined environment. The 3*d* spectrum of Ge exhibits a very broad and featureless line shape from which no structural information can be derived, see Fig. 5(b).

A series of empty- and filled-state STM images (15×15 nm^2) is presented in Figs. 6(a)–6(h), obtained at a temperature of ≈40 K in constant current mode (200 pA). Let us first consider the empty-state images shown in Figs. 6(a)–6(d). At a sample bias of +2.5 V, the surface looks well ordered and shows a clear hexagonal pattern of bright blobs with a diameter of about ≈10 Å, indicating that they correspond to

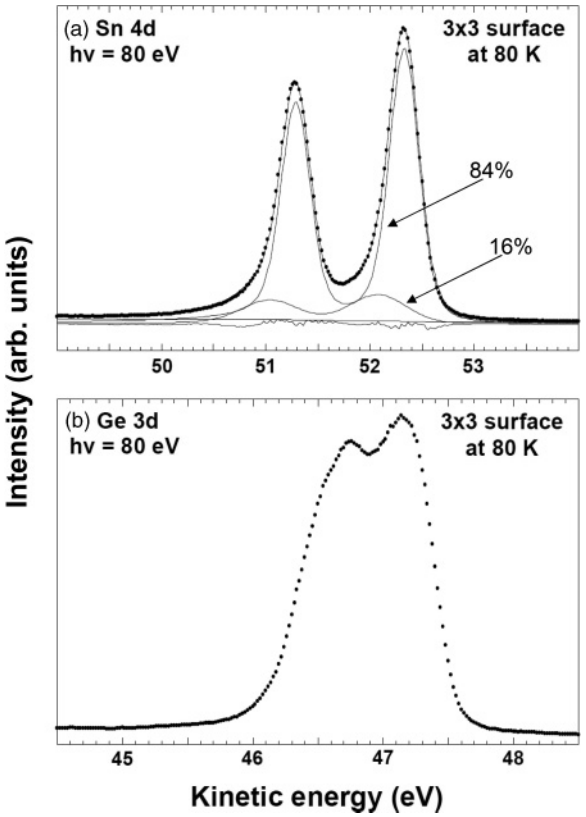

FIG. 5. (a) Sn 4*d* core-level spectrum from the Sn/Ag/Ge(111) 3×3 surface. (b) Ge 3*d* spectrum from the same surface.

clusters of atoms instead of a single atom. Some blobs are slightly less bright, but the shapes are essentially round as for the bright ones. At a bias of +1.5 V, the STM image shows a drastically different appearance. The hexagonal arrangement of protrusions is replaced by a honeycomb structure that looks quite disordered due to a significant variation in the brightness of the periodic features. At a slightly lower bias (+1.3 V), a clearer image of the honeycomb structure is obtained, as shown in Fig. 7(c). At the lower biases, +0.5 and +0.3 V, more details are revealed in the images. The finer corrugation observed at these two biases corresponds to a 1×1 periodicity. In the case of the +0.3 V image, there seems to be a 3×3 corrugation superimposed on the 1×1 structure. The overall impression resembles that of the image obtained at +2.5 V, showing a hexagonal structure. Summarizing the appearances of the empty-state images, one can conclude that the surface shows a hexagonal pattern at high and low biases, while at an intermediate bias, it exhibits a honeycomb structure.

Filled-state images are presented in Figs. 6(e)–6(h). At a bias of −2.5 V, a hexagonal pattern similar to that at +2.5 V is observed. There is, however, a clear difference in that the blobs appear less well ordered, and their shapes are more irregular. The irregular shape of the blobs persists in the −1.5 and −0.5 V images, and the hexagonal structure remains. At the sample bias of −0.3 V, the hexagonally ordered blobs are just barely visible, resulting in an STM image very close to the +0.3 V image. All images in Fig. 6 were obtained from the same area, except for a slight shift, as indicated by the position of the defect near the center of the images. In contrast to the

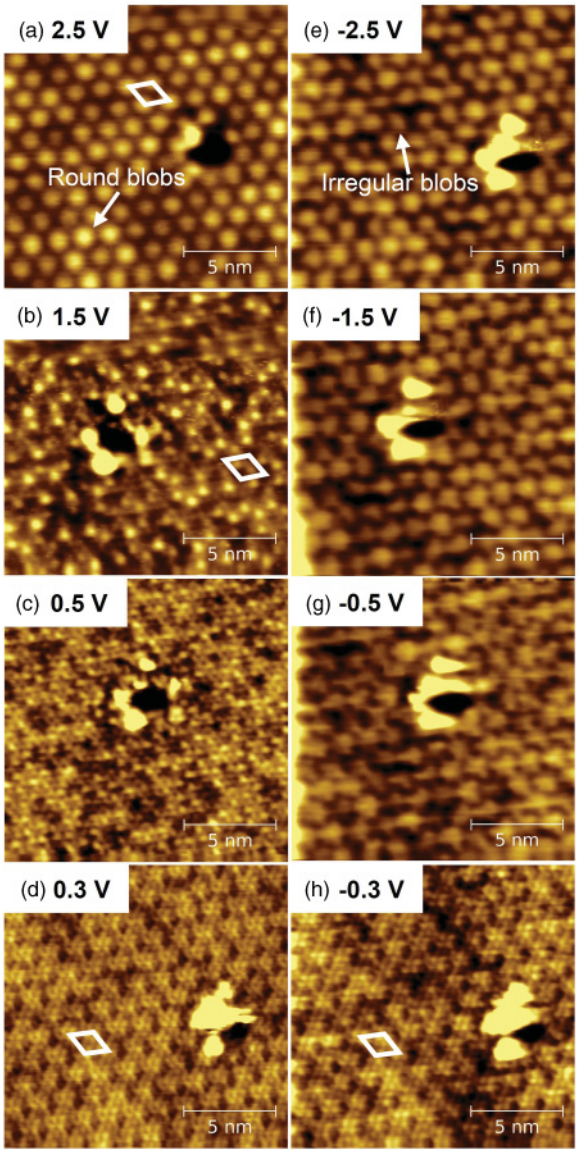

FIG. 6. (Color online) (a)–(d) Empty-state and (e)–(h) filled-state STM images (15×15 nm^2) at different sample biases (±0.3 to ±2.5 V) obtained at a temperature of $\approx$40 K in constant current mode (200 pA). Here, 3×3 unit cells are drawn in (a), (b), (d), and (h).

empty-state images, the filled-state images show a hexagonal pattern at all sample biases.

Figures 7(a)–7(d) show small-area (8.5×8.5 nm^2) STM images of the Ge(111)c(2×8), Ag/Ge(111) $\sqrt{3}\times\sqrt{3}$, and Sn/Ag/Ge(111) 3×3 surfaces. Figures 7(a) and 7(b) were recorded at room temperature, while Figs. 7(c) and 7(d) were obtained at a temperature of $\approx$40 K. Figure 7(a) shows an empty-state STM image of the clean Ge(111)c(2×8) surface used as a substrate for the deposition of Ag. The appearance of the resulting Ag/Ge(111) $\sqrt{3}\times\sqrt{3}$ surface, tunneling to empty states, is shown in Fig. 7(b). This surface exhibits a honeycomb structure, as has been reported in the literature.[20] A similar honeycomb structure, but expanded and rotated by 30°, is shown for the Sn/Ag/Ge(111) 3×3 surface by the empty-state STM image in Fig. 7(c). The $\sqrt{3}\times\sqrt{3}$ and 3×3 unit cells are indicated in Figs. 7(b) and 7(c), respectively. The well-ordered

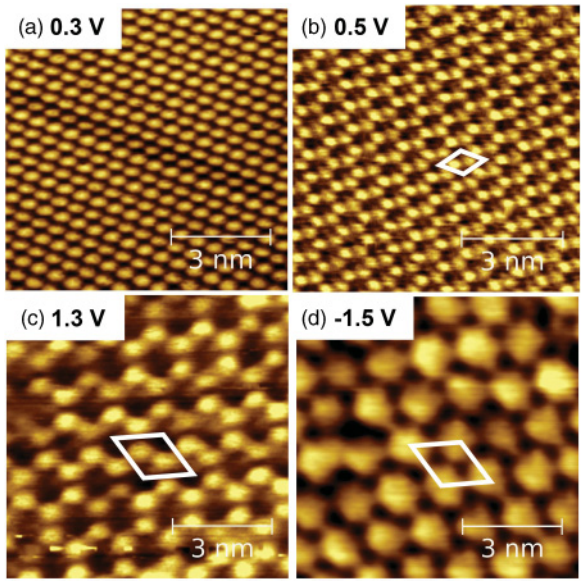

FIG. 7. (Color online) Empty-state STM images of (a) Ge(111)c(2×8) (at 0.3 V), (b) Ag/Ge(111) $\sqrt{3}\times\sqrt{3}$ (at 0.5 V), and (c) Sn/Ag/Ge(111) 3×3 (at 1.3 V). (d) Filled-state image of Sn/Ag/Ge(111) 3×3 (at -1.5 V). A $\sqrt{3}\times\sqrt{3}$ unit cell is shown in (b), and 3×3 unit cells are included in (c) and (d). All images have the same size (8.5×8.5 nm^2).

3×3 empty-state honeycomb structure was recorded at $+1.3$ V, which was found to be the optimum bias voltage to image this structure. The bright small blobs in the empty-state image appear as dark spots in the filled-state image obtained at -1.5 V, Fig. 7(d). In contrast to the empty-state image the filled states exhibit a hexagonal structure. There is one blob per 3×3 unit cell, and the large size indicates that each one represents a cluster of atoms. Based on 1 ML of Ag and 0.75 ML of Sn, one might assign each blob to as many as 15–16 atoms.

IV. SUMMARY

A detailed study has been presented of a well-ordered binary Sn/Ag metallic overlayer on Ge(111)c(2×8) containing 1 ML of Ag and 0.75 ML of Sn. Low-energy electron diffraction showed a sharp 3×3 pattern indicating a high degree of order. The high quality of the surface was further verified by angle-resolved photoelectron spectroscopy, which revealed an extremely detailed surface band structure within the first 1.5 eV below E_F, and by scanning tunneling microscopy, which showed quite a small number of defects. A detailed investigation of the electronic structure of the surface revealed seven bands (S_1', S_1–S_6) that followed the 3×3 periodicity. An additional set of three surface bands (A_1–A_3) were identified that were consistent with a 1×1 periodicity. The large number of surface bands is quite exceptional and, to our knowledge, the only metal on semiconductor system that comes close is Au/Si(111) 6×6, which has eight surface bands in the projected bulk band gap.[27] A detailed analysis of constant energy contours mapped on the 3×3 SBZ explained an intriguing splitting observed in the band structure near E_F. Band dispersions obtained from cuts through the three dimensional (E,k_x,k_y) dataset showed clearly the existence of

two bands. However, the bands are only separated along the $\bar{\Gamma} - \bar{M}$ line of the 3×3 SBZ as illustrated in the summary of the 3×3 surface band structure in Fig. 4. These two surface bands cross the Fermi level and disperse down to -0.40 eV at $\bar{\Gamma}$ and down to -0.30 eV at $\bar{K}$. Although the STM study resulted in high-quality images, the level of detail was not sufficient to derive an atomic structure. The features observed by STM that form the 3×3 structure are quite extended. There is just one such feature per unit cell which implies that it corresponds to a large number of atoms, but no internal structure could be resolved by the STM. Our study has shown that binary metallic overlayers of a high degree of perfection can be formed on Ge(111). This finding acts as inspiration to investigate other binary overlayers on semiconductor surfaces.

ACKNOWLEDGMENTS

Technical support from Johan Adell and T. Balasubramanian at MAX-lab is gratefully acknowledged. Financial support was provided by the Swedish Research Council (VR) and the Knut and Alice Wallenberg Foundation (KAW).

*Corresponding author: sohail@ifm.liu.se

[1] H. W. Yeom, S. Takeda, E. Rotenberg, I. Matsuda, K. Horikoshi, J. Schaefer, C. M. Lee, S. D. Kevan, T. Ohta, T. Nagao, and S. Hasegawa, Phys. Rev. Lett. **82**, 4898 (1999).

[2] J. N. Crain, K. N. Altmann, C. Bromberger, and F. J. Himpsel, Phys. Rev. B **66**, 205302 (2002).

[3] E. Rotenberg, H. Koh, K. Rossnagel, H. W. Yeom, J. Schäfer, B. Krenzer, M. P. Rocha, and S. D. Kevan, Phys. Rev. Lett. **91**, 246404 (2003).

[4] J. L. McChesney, J. N. Crain, V. Pérez-Dieste, F. Zheng, M. C. Gallagher, M. Bissen, C. Gundelach, and F. J. Himpsel, Phys. Rev. B **70**, 195430 (2004).

[5] I. Matsuda, T. Hirahara, M. Konishi, C. Liu, H. Morikawa, M. D'angelo, S. Hasegawa, T. Okuda, and T. Kinoshita, Phys. Rev. B **71**, 235315 (2005).

[6] R. Cortés, A. Tejeda, J. Lobo, C. Didiot, B. Kierren, D. Malterre, E. G. Michel, and A. Mascaraque, Phys. Rev. Lett. **96**, 126103 (2006).

[7] W. H. Choi, H. Koh, E. Rotenberg, and H. W. Yeom, Phys. Rev. B **75**, 075329 (2007).

[8] W. H. Choi, P. G. Kang, K. D. Ryang, and H. W. Yeom, Phys. Rev. Lett. **100**, 126801 (2008).

[9] M. Sasaki, J. Yuhara, M. Inoue, and K. Morita, Surf. Sci. **283**, 327 (1993).

[10] J. Yuhara, M. Inoue, and K. Morita, J. Vac. Sci. Technol. A **11**, 2714 (1993).

[11] J. Yuhara, R. Ishigami, and K. Morita, Surf. Sci. **326**, 133 (1995).

[12] D. Ishikawa, J. Yuhara, R. Ishigami, K. Soda, and K. Morita, Surf. Sci. **356**, 59 (1996).

[13] J. Yuhara, D. Ishikawa, and K. Morita, Appl. Surf. Sci. **117-118**, 94 (1997).

[14] D. Nakamura, J. Yuhara, and K. Morita, Appl. Surf. Sci. **130–132**, 72 (1998).

[15] X. Tong, C. S. Jiang, and S. Hasegawa, Phys. Rev. B **57**, 9015 (1998).

[16] C. Liu, I. Matsuda, H. Morikawa, H. Okino, T. Okuda, T. Kinoshita, and S. Hasegawa, Jpn. J. Appl. Phys. **42**, 4659 (2003).

[17] H. M. Zhang, Kazuyuki Sakamoto, and R. I. G. Uhrberg, Surf. Sci. **532-535**, 934 (2003).

[18] H. M. Zhang, Kazuyuki Sakamoto, and R. I. G. Uhrberg, Phys. Rev. B **70**, 245301 (2004).

[19] J. K. Kim, K. S. Kim, J. L. McChesney, E. Rotenberg, H. N. Hwang, C. C. Hwang, and H. W. Yeom, Phys. Rev. B **80**, 075312 (2009).

[20] L.-W. Chou, H. C. Wu, Y.-R. Lee, J.-C. Jiang, C. Su, and J.-C. Lin, J. Chem. Phys. **131**, 224705 (2009).

[21] R. I. G. Uhrberg and T. Balasubramanian, Phys. Rev. Lett. **81**, 2108 (1998).

[22] F. Ronci, S. Colonna, A. Cricenti, and G. Le Lay, J. Phys. Condens. Matter **22**, 264003 (2010), and references therein.

[23] N. Sato, T. Nagao, and S. Hasegawa, Phys. Rev. B **60**, 16083 (1999).

[24] D. Grozea, E. Bengu, and L. D. Marks, Surf. Sci. **461**, 23 (2000).

[25] I. Razado-Colambo, J. He, H. M. Zhang, G. V. Hansson, and R. I. G. Uhrberg, Phys. Rev. B **79**, 205410 (2009).

[26] A. L. Wachs, T. Miller, T. C. Hsieh, A. P. Shapiro, and T.-C. Chiang, Phys. Rev. B **32**, 2326 (1985).

[27] H. M. Zhang, T. Balasubramanian, and R. I. G. Uhrberg, Phys. Rev. B **66**, 165402 (2002).